Protonation of 5,10,15,20-tetraphenylsapphyrin—identification of inverted and planar dicationic forms

Krystyna Rachlewicz, Natasza Sprutta, Lechosław Latos-Grażyński,* Piotr J. Chmielewski and Ludmiła Szterenberg

Department of Chemistry, University of Wrocław, 14 F. Joliot-Curie St., Wrocław 50383, Poland

5,10,15,20-Tetraphenylsapphyrin ($TPSH_3$, I0) presents an unusual structural skeleton with an inverted pyrrole ring lying opposite to the bipyrrolic unit. The acid–base chemistry of sapphyrin, involving hydrogen chloride, dichloroacetic acid or trifluoroacetic acid in chloroform, dichloromethane (293 and 203 K) and DMSO (293 K) has been followed by means of UV–VIS electronic and ^1H NMR spectroscopy. The protonation of $TPSH_3$ proceeds stepwise *via* a mono- and a variety of di-cationic forms. The mono-protonated species (I1) preserves the inverted skeleton of I0. Two fundamental structures, inverted (I2) and expanded (P2), have been detected in the case of dications. The transformation of the macrocycle involves a reversible flip of a single pyrrole unit which relocates the 27-NH pyrrolic nitrogen between the periphery and the centre of macrocycle (I⇌P). The rearrangement is triggered by proton and/or anion addition and involves binding of anion(s) *via* a system of multiple NH-anion hydrogen bonds. The sequence of structural transformation is solvent dependent: I0→I1→P2→I2 in dichloromethane (chloroform) but I0→I1→I2→P2 in DMSO for all investigated acids.

A rational formal extension of porphyrin using fundamental building blocks simply involves the insertion of one pyrrole ring between the *meso*- and α-carbons of the porphyrin skeleton, creating a pentapyrrolic macrocycle—sapphyrin. Such a molecule is considered to be the simplest member of the expanded porphyrin class.[1] Sapphyrin is aromatic and possesses an overall 22 π-electron annulene framework. Decaalkyl-substituted sapphyrin was serendipitously discovered by Woodward and co-workers in their effort to synthesise vitamin B_{12}.[2,4] The synthetic procedures, subsequently developed by Brodhurst *et al.*,[3] Bauer *et al.*[4] and Sessler *et al.*,[5] require preorganized substrates and involve a MacDonald-type [3 + 2] condensation between a functionalized bipyrrole and a dicarboxyl-substituted dipyrrane. At present spectroscopic properties of sapphyrins are of particular interest because of their potential application in photodynamic therapy (PDT)[6,7] as they absorb light in the 680–710 nm spectral region,[3–5] *i.e.* at significantly longer wavelengths than the hematoporphyrin derivative currently used in PDT treatment, which absorbs at 630 nm. Such a property is a prerequisite for a new generation of photosensitizers to be able to achieve a greater depth of light penetration.[8]

In the course of systematic investigations of the properties of decaalkyl derivatives of sapphyrin Sessler and co-workers discovered a unique feature of protonated sapphyrins, specifically that they act as efficient anion acceptors both in solution and in the solid state.[5,9–11] The binding of the halide anions,[5,6,9] azide,[10] phosphate and its derivatives,[11] and carboxylate [12] was explored. It was also found that sapphyrins act as solution-phase carriers for nucleotides,[13] nucleotide analogues [14] and amino acids.[15] Unlike neutral polyalkylated sapphyrins, where the X-ray structures are not available, the mono- and di-cations have been structurally characterized.[1,5,9–11] They demonstrate typically a roughly planar arrangement with the pyrrole nitrogens pointed towards the centre of the macrocycle. Depending on their size, the anions are held in the plane of sapphyrin (F^-) or are complexed above the macrocycle plane (Cl^-, N_3^-).[6,9,10] The azide is bound in an end-on-manner with the terminal nitrogen located above the sapphyrin plane. Diprotonated sapphyrins are capable of acting as receptors of biologically important anions—phosphates, including nucleotide monophosphate.[11] Typically only a single oxygen of the phosphate moiety is displaced from the five-nitrogen plane and forms hydrogen bonds with some of the NH protons of diprotonated sapphyrin. The number of hydrogen bonds to oxygen is determined by the properties of the phosphate unit. Altogether, decaalkyl derivatives of sapphyrin provided a new important addition to the family of anion-selective complexing agents.[16,17]

In our search for the macrocyclic products formed in the Rothemund synthesis, we have reported that the condensation of the pyrrole and benzaldehyde yields, apart from tetraphenylporphyrin [18] and inverted tetraphenylporphyrin,[19,20] a pentapyrrolic macrocyclic molecule with an aromatic sapphyrin nucleus, namely 5,10,15,20-tetraphenylsapphyrin ($TPSH_3$).†[21] To account for the spectral characteristics of $TPSH_3$ we have been forced to introduce an unorthodox structural skeleton for 5,10,15,20-tetraphenylsapphyrin. The C pyrrole ring, opposite to the bipyrrole unit, is inverted in a novel configuration.

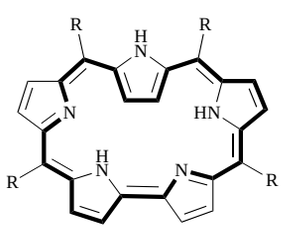

The addition of two equivalents of acid to the dichloromethane solution of $TPSH_3$ resulted in the formation of the diprotonated species $TPSH_5^{2+}$ and acted as the trigger of a profound structural transformation which involves a flip of the pyrrole C. This rearrangement moves the 27-NH pyrrolic nitrogen from the periphery into the centre of the macrocycle. This type of dication contains a central core in which there is a

† Abbreviations used: $TPSH_3$, 5,10,15,20-tetraphenylsapphyrin; 2-NCH_3CTPPH, 2-methyl-5,10,15,20-tetraphenyl-2-aza-21-carbaporphyrin; TPP ($TPPH_2$), 5,10,15,20-tetraphenylporphyrin dianion; TFA^- (TFAH), anion of trifluoroacetic acid; DCA^- (DCAH), anion of dichloroacetic acid.

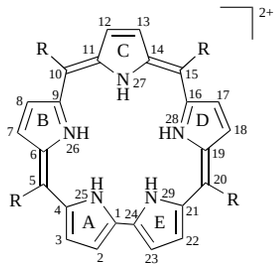

hydrogen atom attached to each of the five inner-crevice nitrogen atoms.

Here we sought to extend our previous investigation, which was concentrated mostly on the identification of the novel macrocycle, by looking at the acid–base chemistry of 5,10,15,20-tetraphenylsapphyrin involving hydrogen chloride, dichloroacetic acid and trifluoroacetic acid, with the aim of elucidating the mechanism of protonation. In particular we have searched for the alternative molecular configurations which might coexist in different protonation stages.

Results and discussion

Spectroscopic criteria for $[TPSH_{3+n}]^{n+}$ identification

The complete description of the $TPSH_3$ acid–base equilibria should be analysed in the context of the feasible inverted and extended sapphyrin core configurations. These two fundamental configurations have been previously detected for 5,10,15,20-tetraphenylsapphyrin although for different protonation states, *i.e.* inverted for neutral $TPSH_3$ (**I**0) and expanded for dicationic $TPSH_5^{2+}$(**P**2). To simplify the description of the equilibria we will refer to the particular cationic species by defining their idealized geometry, *i.e.* **I***n* for inverted and **P***n* for approximately planar species, respectively, with an overall cationic charge equal to $n+$.

The original ^{1}H NMR studies of $TPSH_3$ provided very useful and potentially unique ^{1}H NMR probes for detecting the macrocycle structure.[21] In particular it includes a spectacular upfield⇌downfield jump of the 27-NH and 12,13-H pyrrole resonances, resulting from the molecular rearrangement and relocation of these protons between shielding/deshielding zones of the aromatic macrocycle. The extraordinary upfield position of the 12,13-H pyrrole proton (−1.21 ppm) associated with the very large downfield position of the 27-H resonance (11.75 ppm, $TPSH_3$) set the appropriate shift limits for such a geometry in any protonation stage. Therefore such a pattern will serve as an unambiguous 'fingerprint' of the inverted structure. The roughly planar geometry has been exemplified here by $TPSH_5^{2+}$, which is produced as the dominant ion by addition of exactly two equivalents of TFAH. This dication demonstrates the regular porphyrinic shifts of the crucial resonances (27-NH: −1.98 ppm; 12,13-H: 8.50 ppm). Consequently the 27-NH resonance joins the group of the inner NH resonances to produce an analytically useful 2:1:2 pattern. Of course the multiplicity of the resonances can be altered due to the expected tautomeric equilibria for the neutral and monocationic species although the basic principles of their ^{1}H NMR identification will remain unchanged. The rearrangement **I***n*⇌**P***n* modifies strongly the aromatic chromophore of sapphyrin so the titration can be efficiently followed by electronic spectroscopy, providing a straightforward correlation between the molecular structure and the electronic spectra.

Molecular modelling of sapphyrin dications

In the course of our present investigations we have found that the two structurally different dicationic forms, roughly planar and inverted, do coexist in solution. Their relative concentration has been easily controlled merely by changes of the counteranion concentration. Previously molecular mechanics calculations were carried out for $TPSH_3$ (**I**0) and $TPSH_5^{2+}$ (**P**2) to obtain adequate molecular models of these two fundamental geometric configurations which are accessible in the course of $TPSH_3$ protonation. Here we have carried out the quantum-mechanic calculations for dicationic sapphyrin in two alternative states, planar and inverted, using the GAUSSIAN94 program.[22] For the sake of simplicity the *meso*-phenyl rings of tetraphenylsapphyrin have been replaced by protons. The single point energy calculations were carried out with the Becke–Lee–Yang–Parr composite exchange-correlation functional[23] as implemented in GAUSSIAN94 and the 6-31G** basis set on a structure previously optimized with B3LYP theory and the 3-21G basis set. The results of the calculations have been used to visualize the structures of two alternative dications as presented in Fig. 1. The position of the C pyrrole ring is apparent in the side view of the two different dication configurations. All bond lengths and angles are within the limits expected for porphyrins or sapphyrin.[1,5,9–11,24]

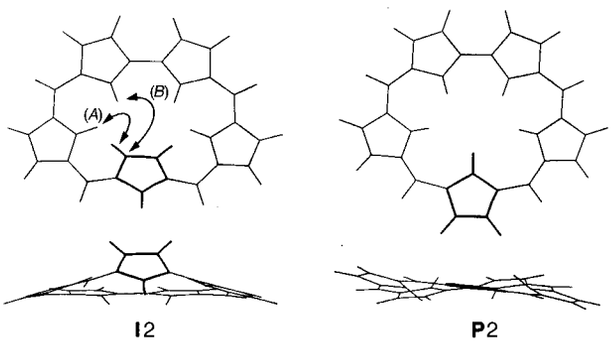

Fig. 1 Drawing of the optimized dication sapphyrin structure as obtained from quantum mechanic calculations by the B3LYP/6-31G**//B3LYP/3-21G method. Projections illustrate the difference of pyrrole arrangements in **I**2 and **P**2. (Arrows indicate the selected through-space contacts observed *via* NOE, see Fig. 4).

The inverted pyrrolic ring of **I**2 is bent out of the plane of the four inner sapphyrin nitrogens. The small folding of the remaining part of the macrocycle has been determined. The extent of distortion, reflected by a dihedral angle $C^9C^{10}C^{11}C^{12}$, equals 31.6° for **I**2 compared with 175.9° for **P**2. The strong distortion of **I**2 from planarity still allows the 22 π-electron delocalization of sapphyrin. The **P**2 structure shows modest buckling of the sapphyrin macrocycle. This dication has C_2 symmetry with the main C_2 axis passing through the N^{27} atom, and through the centre of the C^1–C^{24} bond. The inverted form is only slightly less stable than the planar one. Thus the relative energy of **I**2 with respect to **P**2 as obtained by the B3LYP/6-31G**//B3LYP/3-21G method equals 27.06 J mol^{-1}.

Generally these values are comparable with those expected for typical hydrogen bonds. Accordingly we suggest that chelation of the anion by the dication of sapphyrin *via* formation of multiple N–H–X hydrogen bonds plays a crucial role in selection of the appropriate geometry of the macrocycle involved. Therefore, the stabilization of the hydrogen bond network may dominate selection of the appropriate configuration.

Protonation of $TPSH_3$ with TFAH in dichloromethane and chloroform

Titration of $TPSH_3$ with TFAH as observed by electronic spectroscopy in dichloromethane, is presented in Fig. 2. Two discrete stages of a process corresponding to the dicationic species $TPSH_5^{2+}$ **P**2 and **I**2 have been detected. The electronic spectrum of **I**0 shows a split Soret-like band at 493 and 518 nm accompanied by four *Q* bands at 640, 697, 710 and 790 nm. The formation of **P**2 results in some simplification of the spectrum which presents the Soret-like band at 485 nm and two *Q* bands at 650 and 740 nm. With the formation of **P**2 we observe the disappearance of the band at 790 nm which seems to be diag-

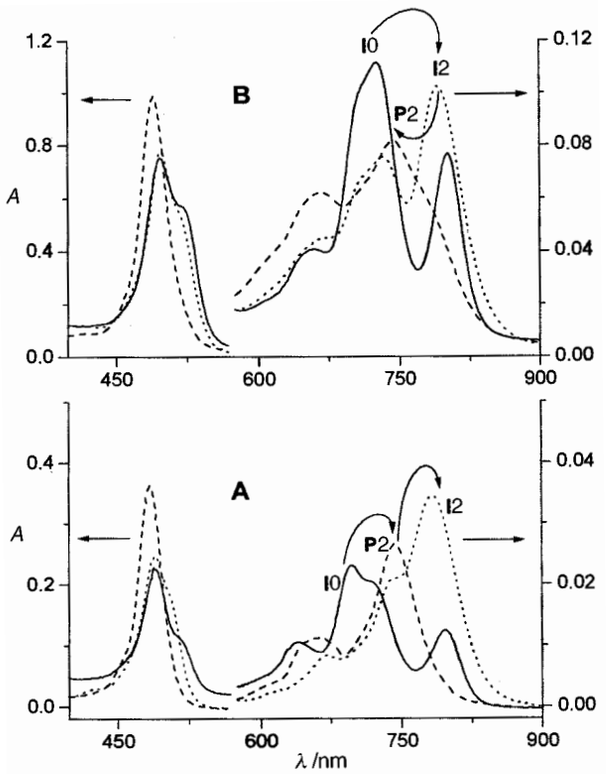

Fig. 2 (A) Electronic spectra of $TPSH_3$ dichloromethane solutions obtained in the course of titration with TFAH at 293 K; (——) $TPSH_3$–**I**0; (– – –) $TPSH_5^{2+}$–**P**2; (···) $TPSH_5^{2+}$–**I**2; (B) Electronic spectra of $TPSH_3$ in DMSO solutions obtained in the course of titration with TFAH at 293 K; (——) $TPSH_3$–**I**0; (– – –) $TPSH_5^{2+}$–**P**2; (···) $TPSH_5^{2+}$–**I**2. The cationic species are formed in different sequences in two solvents: **I**0→**P**2→**I**2 in dichloromethane but **I**0→**I**2→**P**2 in DMSO as marked by arrows at the respective traces.

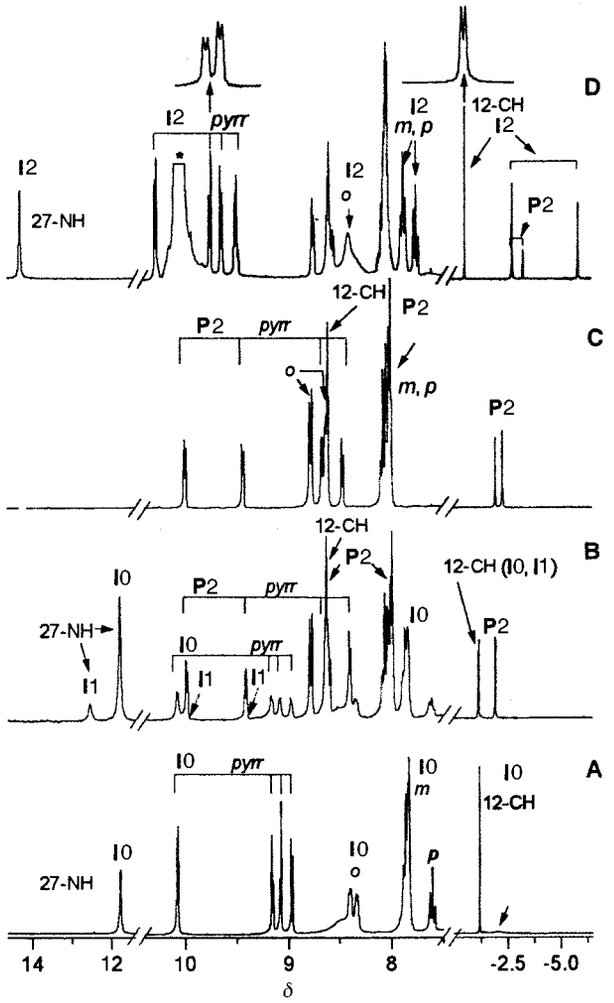

Fig. 3 ^1H NMR spectra (300 MHz) of $TPSH_3$ in [^2H]chloroform at 293 K: (A) spectrum of $TPSH_3$ alone; (B) spectrum after addition of 1 equiv. of TFAH; (C) spectrum after addition of 2 equiv. of TFAH; (D) spectrum after addition of 50 equiv. of TFAH. Inset at trace D shows the representative example of the four-bond $^4J_{HH}$ coupling between β-CH and NH protons observed for all pyrrolic protons of **I**2. Resonances due to individual species are denoted as described in the text according to their geometry and degree of protonation. The specific resonance assignments, if given, follow the systematic numbering of the sapphyrin skeleton: *pyrr*, pyrrole; phenyl resonances: *o*, ortho; *m*, meta; *p*, para. The structure marker resonances 27-NH and 12-CH are separately labelled. All resonances in the 0 to −6 ppm region are assigned to NH protons unless labelled differently. The relative intensity of the 0 to −6 ppm and 11 to 15 ppm regions are enhanced to show peaks of the species formed in a small amount.

nostic of the **I***n* type molecular structure. The further addition of TFAH (the 1 : 50 molar ratio) produced notable changes in the long wavelength region. In particular the strong *Q*-type band re-emerged at 780 nm accompanied by two other *Q* bands at 670 and 740 nm. The Soret-like band [490, 510 (sh) nm] is slightly bathochromically shifted with respect to **P**2. Accordingly the **I**2 geometry can be identified based solely on the UV–VIS titration. We have carried out the analogous UV–VIS experiment at 203 K, confirming an identical sequence of events in the course of protonation, although the formation of **I**2 has been detected for a relatively smaller concentration of TFAH.

The individual resonances of neutral **I**0, monocationic **I**1 and two dicationic species **P**2 and **I**2 have been concurrently identified during the parallel ^1H NMR titration (Figs. 3 and 4). These observations have been attributed to a slow exchange among ionic forms in the system under the conditions of our experiment. The unambiguous assignment of **I**0 and **P**2 resonances has been previously achieved by selective deuteration of the 5,10,15,20-phenyl groups ([$^2H_{20}$]$TPSH_3$), an exchange of labile NH protons ($TPSH_3$) by deuterons ($TPSD_3$) in the presence of D_2O, and by 2D ^1H NMR COSY and NOESY experiments carried out at 203 K in [$^2H_2$]dichloromethane.[21] A similar approach has been applied here to assign resonances of newly identified **I**1 and **I**2 forms (Figs. 3 and 4). Their ^1H NMR spectra resemble roughly the spectrum of neutral **I**0. For instance, two sets of doublets of doublets of 2,3-H and 7,8-H for **I**2 are located in the downfield region (Fig. 3, trace D). The inverted structure markers 27-NH and 12,13-H (doublet) are appropriately located in the downfield (14.3 ppm) and upfield (−0.57 ppm) regions. The fine splitting of all pyrrole resonances into doublets ($^4J_{HH}$ = 1.5 Hz) reflects scalar coupling between pyrrole and NH protons located on the same five-membered ring (Fig. 3, two insets in trace D) and disappears for the N-deuterated samples. Four inner NH protons of **I**2 exhibit two upfield shifted singlets easily distinguished from the upfield located 12,13-H line by means of selective deuteration during the course of titration with TFAD. Analogous $^4J_{HH}$ coupling has also been seen here for the **P**2 form. The diprotonated **I**2 species remains aromatic. All outer pyrrole and *meso*-phenyl resonances are strongly downfield shifted due to the ring current effect. The remarkable shift differences between the outer and inner CH ($\Delta\delta$ = 9.17) and NH ($\Delta\delta$ = 12.01) pyrrolic protons support this conclusion. The rotation of the 10,15-phenyl rings is slow below 213 K giving two well-separated *ortho* resonances and two well-separated *meta* resonances (Fig. 4, trace D). These resonances coalesce above 213 K producing a broad line at the averaged position (8.38 ppm, 293 K). Such a differentiation of *ortho* and *meta* resonances can be accounted for by the markedly folded structure of the sapphyrin nucleus rendering the two sides of the macrocycle non-equivalent, as has been determined for **I**0. The considerable difference in the

Table 1 Selected ^{1}H NMR data for $TPSH_3$ and its protonated forms[a]

Proton assignment	**I**0[b]	**I**0[c]	**I**1[b] (HCl)	**P**2[b] (HCl)	**P**2[b] (TFAH)	**P**2[b] (DCAH)	**I**2[b] (HCl)	**I**2[c] (TFAH)
2, 23	10.055	10.15	9.98	10.30	10.00	10.00	10.30	10.24
3, 22	9.137	9.20	9.31	9.55	9.45	9.42	9.76	9.80
7, 18	8.945	9.02	9.20	8.96	8.47	8.43	9.65	9.73
8, 17	9.057	9.15	9.15	9.18	8.67	8.65	9.52	9.43
12, 13	−1.281	−1.50	−1.38	8.86	8.62	8.62	−0.57	−0.79
25-NH, 29-NH	−1.9(b)	−2.58	−2.28	−2.61	−1.96	−1.37	−2.79	−2.45
26-NH, 28-NH	−1.9(b)	−2.58	−2.28	−3.56	−2.29	−1.95	−5.89	−6.09
27-NH	11.767	12.24	12.41	−2.74	−2.29	−2.04	14.30	14.80

[a] All chemical shifts relative to TMS. Positions of all resonances, specially 12-CH and NH, strongly depend on the acid concentration. Shifts given for the $TPSH_3$: acid molar ratio are 1 : 2 for **P**2 and 1 : 50 for **I**2. [b] $CDCl_3$, 293 K. [c] CD_2Cl_2, 203 K.

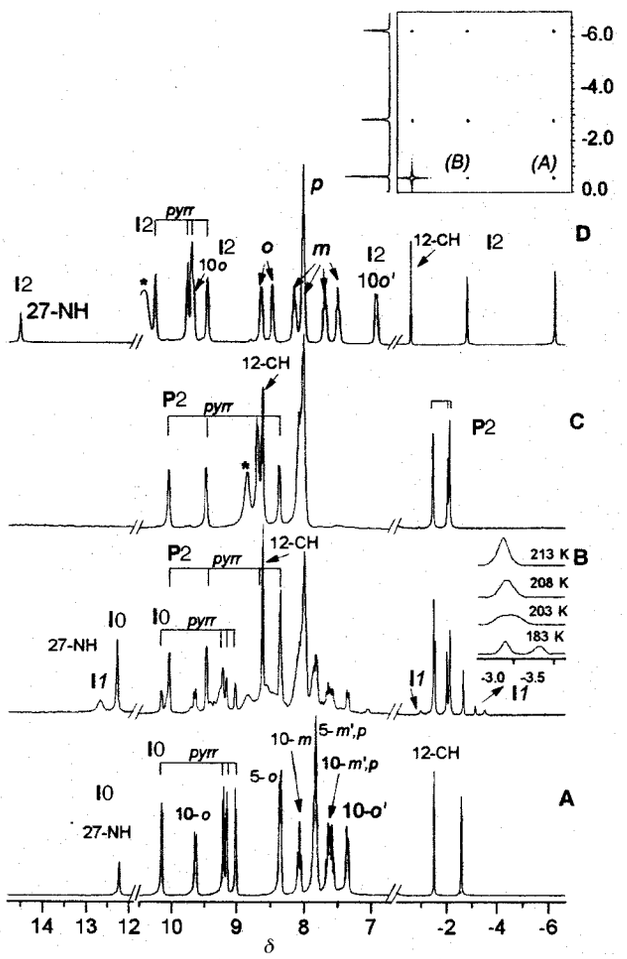

Fig. 4 ^{1}H NMR spectra (300 MHz) of $TPSH_3$ in [$^2H_2$]dichloromethane: (A) spectrum of $TPSH_3$ alone at 203 K; (B) spectrum after addition of 1.5 equiv. of TFAH at 183 K. The inset at trace B presents the temperature dependence of the upfield NH pattern; (C) spectrum after addition of 2 equiv. of TFAH at 203 K; (D) spectrum after addition of 40 equiv. of TFAH at 203 K. Inset at trace D presents the selected part of the ^{1}H 2D NOESY map obtained for the sample used in the experiment (D). Cross-peaks connecting 12-H and 26-NH and 25-NH resonances due to dipolar coupling are shown. Labelling of resonances as described in Fig. 2. * The TFA*H* resonance. The relative intensity of the 0 to −6 ppm and 11 to 15 ppm regions are enhanced to show peaks of the species formed in a small amount.

2-H and 3-H chemical shifts is common for $TPSH_{3+n}^{n+}$ (n = 0,1,2) and reflects the upfield ring current contribution of the 5-phenyl ring available for the 3-H but not for the 2-H proton.

The final determination of the dication **I**2 structure results from the two-dimensional NOESY experiment carried out at the lower temperature limit in order to stabilize the position of the otherwise rotating 10,15-phenyls. The analysis of the NOESY map (Fig. 4) revealed the following cross peaks fundamental for the structure determination: 12-H–26-NH (A) , 12-H–25-NH (B), [the assignment of the cross peaks at the NOESY map is given in parentheses, the corresponding (A) and (B) spatial contacts are shown in Fig. 1]. Such a spatial proximity is attainable exclusively for the sapphyrin skeleton with an inverted structure. In addition we have noticed the differentiation of the A and B cross-peak intensities (A > B). This fact reflects the difference in the distances between 12-H and the inner NH protons, as measured from the respective molecular model, confirming their unambiguous identification (Table 1).

Thus the description of the **I**2 species, accomplished by UV–VIS and ^{1}H NMR spectroscopy, has reached the level obtained for **I**0. On the other hand, the spectroscopic characterization of a monocation **I**1 has been hampered by the fact that this cation is formed in minute amounts compared to other species, *i.e.* **I**0 and **P**2, coexisting in dichloromethane solution in any concentration of TFAH. The electronic spectrum of **I**1 is practically covered by **I**0 and **P**2 bands. However, we could take full advantage of ^{1}H NMR spectroscopy by using two transparent ^{1}H NMR windows at the 15–10 and 0 to −6 ppm spectral ranges. We have identified (Fig. 4, trace B) the following marker resonances: 27-NH, 12.5 ppm; 12,13-H, −1.14 ppm (293 K) and 27-NH, 12.67 ppm; 12,13-H, −1.54 ppm (203 K) (detected unambiguously using TFAD) and three inner NH −3.21, −3.50, −0.98 ppm at 183 K. In addition we could distinguish some pyrrole resonances at 10.1 and 9.3 ppm as well as the analytically important 10-*o* resonance at 9.7 ppm. Thus the ^{1}H NMR analysis of **I**1 is consistent with the inverted sapphyrin core. The general mechanism of protonation, which includes the relevant tautomeric equilibria of the monoprotonated species is presented in Scheme 1.

Tautomeric equilibria of I1

In contrast to tetraphenylporphyrin[25] and its β-substituted derivatives[26] but similarly to porphycene,[27] tetraphenylsapphyrin $TPSH_3$ **I**0 demonstrated an extremely fast NH tautomerism even at −90 °C due to the rapid exchange of two imino protons between four structurally non-equivalent internal nitrogens of sapphyrin.[21] The outer 27-NH was not involved in the process. We have previously demonstrated that the equilibrium corresponds to the exchange between two degenerate asymmetric **I**0 tautomers.[21] The first addition of one proton to **I**0 can produce two types of structures. Considering the symmetry of the system the complex equilibria can be considered at this protonation level (Scheme 1). Pairs of enantiomeric tautomers, $\mathbf{I}1_a$–$\mathbf{I}1_{a'}$ or $\mathbf{I}1_b$–$\mathbf{I}1_{b'}$, would not be distinguishable by means of ^{1}H NMR spectroscopy. On the other hand tautomers $\mathbf{I}1_a$ and $\mathbf{I}1_b$ should be easily differentiated. At the slow exchange limit one can expect three inner NH resonances for each tautomeric form. They should be accompanied by twice the number of resonances for each sapphyrin position when compared to the fast exchange limit. The hypothetically complicated situation reveals, however, the relatively simple spectral pattern. The number of pyrrole resonances is the same

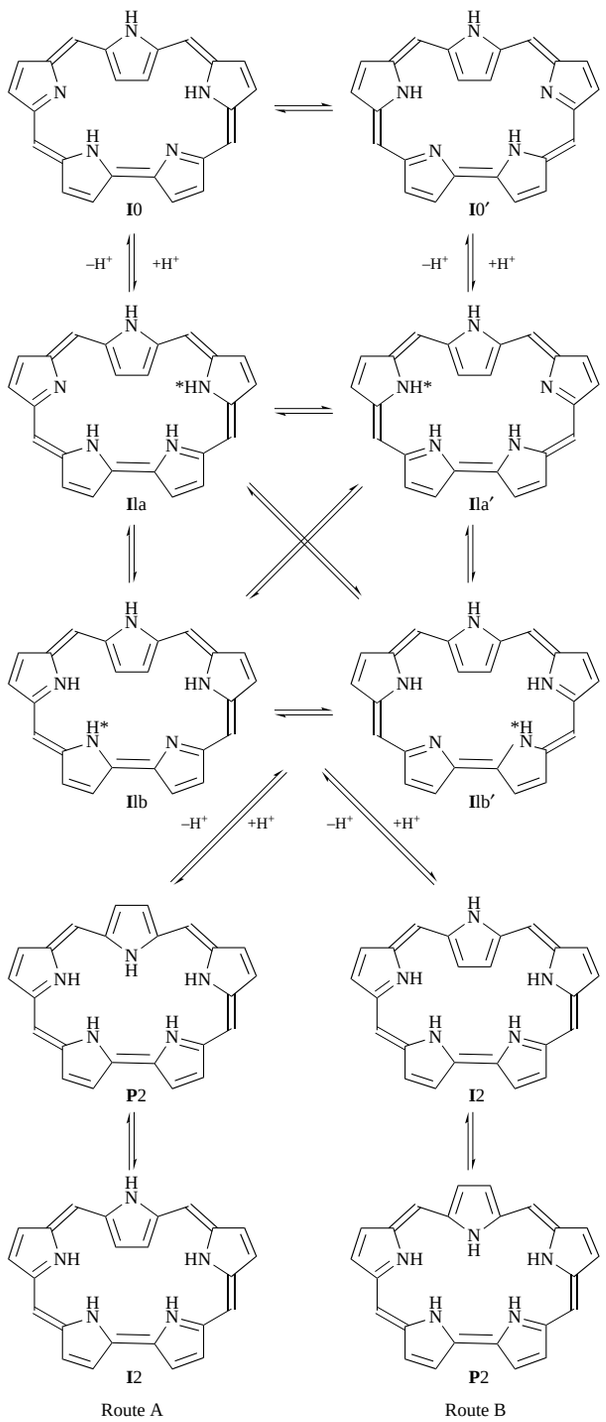

Scheme 1

as that for **I**0. This observation implies the fast exchange of the inner NH protons, although this is contradicted by the more complex behaviour observed in Fig. 4 (inset in trace B). At 293 K we have identified a single broad NH resonance with carefully measured intensity corresponding to two protons. The third proton resonance was apparently too broad to be observed in this temperature. In the low temperature experiments (183–203 K) we have detected three inner NH resonances. Evidently the two-proton singlet seen at −3.12 ppm (213 K) splits into two well-separated lines below the coalescence temperature due to lowering of the exchange rate (−3.11, −3.43 ppm, at 183 K). In addition these resonances are relocated slightly upfield upon lowering the temperature. Furthermore, the third resonance is observed at −1.03 ppm. To account for the spectral behaviour we assume that only one enantiomeric couple of tautomers is predominant in the solution so we are dealing either with $\mathbf{I}1_a \rightleftharpoons \mathbf{I}1_{a'}$ or $\mathbf{I}1_b \rightleftharpoons \mathbf{I}1_{b'}$ equilibria. The fast exchange between all feasible tautomers would produce a single NH line of three-proton intensity. Although the exchange is slow enough for NH protons to be differentiated it is still sufficiently fast to produce an averaged spectrum for all CH protons. Presumably the shift difference between two external situations in the internally asymmetric **I**1 is relatively small for CH protons as compared to NH ones. Accordingly for the same process we observe different dynamic windows depending on the spectroscopic probe. At present we are not able to distinguish between the two alternative equilibria. To account for the dynamic behaviour detected here by ^{1}H NMR spectroscopy, only one of the three inner NH protons can move inside the sapphyrin core. Additionally this step will produce exclusively a single species which is enantiomeric to the starting one. Accordingly the exchange between A and E or B and D pyrrolic rings (depending on the tautomeric pair) is allowed. Any exchange between A and B or D and E should produce a single three-proton resonance. Thus the following exchanges are feasible: (25-NH, 26-NH, 28-N, 29-NH) and (25-NH, 26-N, 28-NH, 29-NH) or (25-N, 26-NH, 28-NH, 29-NH) and (25-NH, 26-NH, 28-NH, 29-N). In Scheme 1 this condition has been taken into account and the proton involved has been marked by an asterisk.

Protonation of $TPSH_3$ with TFAH in [$^2H_6$]DMSO

To investigate the influence of the solvent polarity on the protonation mechanism we have carried out the titration of $TPSH_3$ also with TFAH but in [$^2H_6$]DMSO. The UV–VIS experiment and parallel ^{1}H NMR titrations are illustrated in Fig. 2 (trace B) and Fig. 5. The spectral analysis, following the methods for titrations carried out in chlorinated solvents, resulted in the resonance assignments shown in Fig. 5. The inner NH protons are not visible in the ^{1}H NMR spectra due to exchange with the residual D_2O from the solvent. The ^{1}H NMR data of the starting material are consistent with **I**0 structures so the change of solvent polarity has not influenced the neutral form geometry. However, the first formed dicationic species reveals features assigned definitely to **I**2. Only an addition of TFAH in excess triggers the structural rearrangement converting **I**2 into **P**2. We have also noticed that the addition of the first proton to produce **I**1 can be inferred from the untypical behaviour of the spectral pattern. We have followed the diminishing intensity of **I**0 accompanied by the formation of a set of broad resonances which finally narrowed for a 1:2 molar ratio of $TPSH_3$ to TFAH to the **I**2 spectrum. To account for this behaviour we assumed an intermediate rate of exchange between **I**1 and **I**2 which produces the averaged shift for the protons of the two species under consideration although still causing the severe broadening of all new resonances. We suggest that the addition of the first proton modifies the inverted structure of **I**0. On the other hand **I**1 and **I**2 seem to be more alike, facilitating faster exchange between **I**1 and **I**2 where the separate resonances of **I**0 are detected over the whole titration range. The ^{1}H NMR detected mechanism is consistent with the electronic spectra. In particular, the intensity of the 790 nm band, *i.e.* the indicator of the **I**2 geometry, diminishes at high acid concentration. Thus in [$^2H_6$]DMSO we have detected all the previously identified ionic species. They are formed in the solvent dependent order **I**0→**I**1→**P**2→**I**2 in dichloromethane (route A in Scheme 1) but **I**0→**I**1→**I**2→**P**2 in DMSO (route B in Scheme 1).

Protonation of $TPSH_3$ with DCAH

We have tested the suggested dissociation mechanism in the parallel titration of $TPSH_3$ with DCAH, which is a weaker acid. The process has been followed by UV–VIS electronic spectroscopy (not shown) revealing an identical spectroscopic sequence to that of TFAH. Thus the general scheme of the protonation by DCAH resembles the $TPSH_3$–TFAH system in dichloromethane.

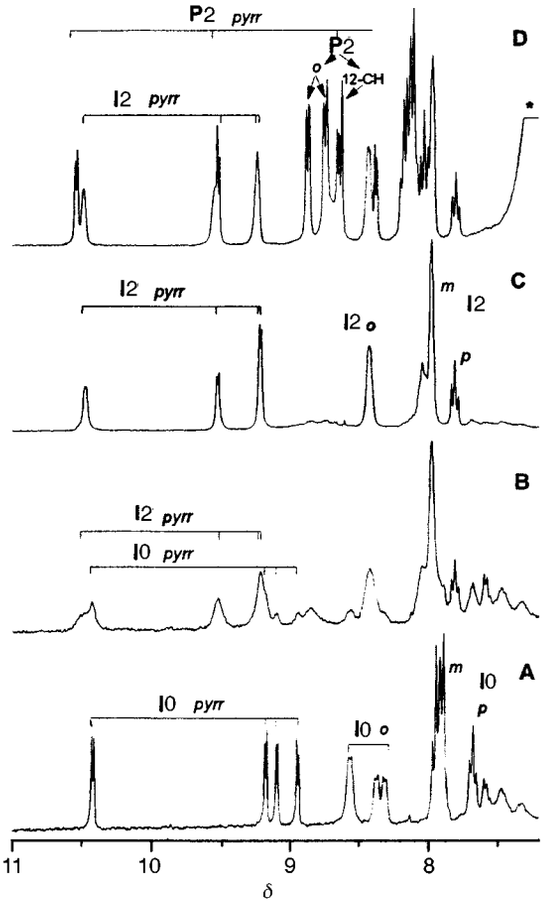

Fig. 5 ^{1}H NMR spectra (300 MHz) of $TPSH_3$ in [$^2H_6$]DMSO at 293 K: (A) spectrum of $TPSH_3$ alone; (B) spectrum after addition of 0.3 equiv. of TFAH; (C) spectrum after addition of 2 equiv. of TFAH; (D) spectrum after addition of 50 equiv. of TFAH. Labelling of resonances as described in Fig. 2. The upfield located resonances of 12,13-CH (**I**0, **I**2) are not shown.

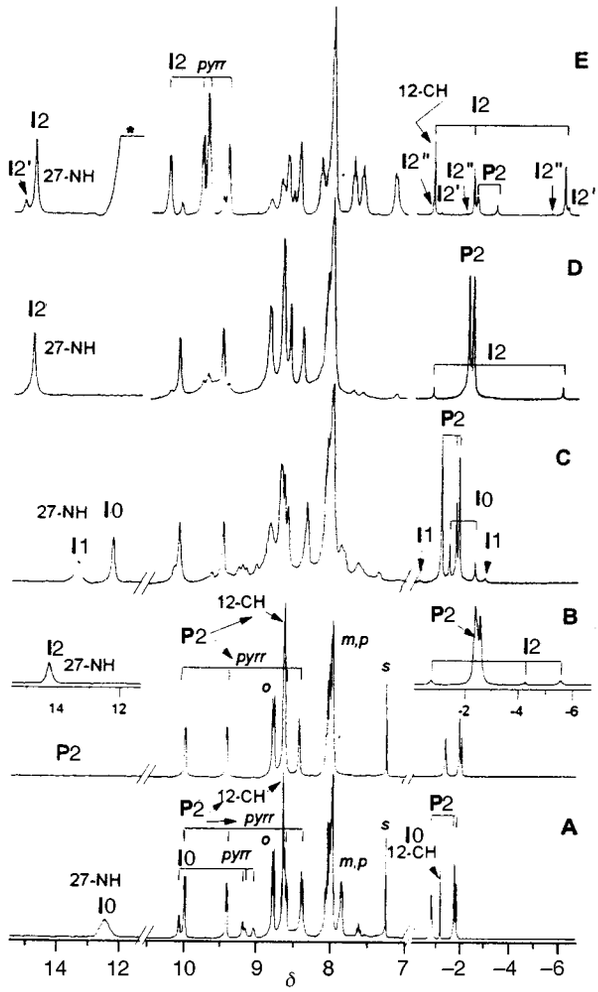

Fig. 6 ^{1}H NMR spectra (300 MHz) of $TPSH_3$: (A) spectrum after addition of 1 equiv. of DCAH ([^{2}H]chloroform, 293 K); (B) spectrum after addition of 2 equiv. of DCAH ([^{2}H]chloroform, 293 K); Inset at trace B presents the evidence for the formation of **I**2 in the presence of 50 equiv. of DCAH at 293 K; (C) spectrum after addition of 1 equiv. of DCAH ([$^2H_2$]dichloromethane, 203 K); (D) spectrum after addition of 2 equiv. of DCAH ([$^2H_2$]dichloromethane, 203 K); (E) spectrum after addition of 65 equiv. of DCAH ([$^2H_2$]dichloromethane, 203 K); labelling of resonances as described in Fig. 2. The relative intensity of the 0 to −6 ppm and 11 to 15 ppm regions are enhanced to show peaks of the species formed in a small amount.

The dichloromethyl group of DCAH/DCA^- allowed investigation of the structure of the cationic forms by using the anion resonance(s) as an independent ^{1}H NMR spectroscopic probe. The neutral, monocationic and two dicationic forms, created in the sequence **I**0→**I**1→**P**2→**I**2, showed separate spectra (Fig. 6). The **I**1 form has been identified only at low temperature (Fig. 6, trace C). The essential differences in the chemical shifts and spectral patterns (Table 1), observed between **I***n* and **P***n* generated by TFAH and DCAH, reflect the existence of tight ionic pairs. These observations point to the influence of the anion on the detailed structure of ionic aggregates. The C*H*Cl_2 resonance of a bonded DCA^- anion has been identified at 1.38 ppm at the first stage of titration up to the 1 : 2 sapphyrin–DCAH molar ratio. The single averaged resonance of C*H*Cl_2, corresponding to fast exchange between coordinated and non-coordinated DCA^-/DCAH molecules, has been observed. This resonance moved gradually downfield, *i.e.* in the direction of the free acid position, as the molar ratio of $TPSH_3$ to DCAH increased. Its permanently upfield position with respect to free DCAH reflects plainly the contribution of the aromatic ring current shielding effect in the averaged shift of C*H*Cl_2 and its location in the deshielding zone of the sapphyrin macrocycle. The gradual addition of DCAH is accompanied by the consistent upfield shift of the inner NH protons of the **P**2 form, which exists exclusively if 2 to 20 equivalents of acid are available. Finally, at a $TPSH_3$–DCAH molar ratio of 1 : 50, the **I**2 form occurs.

A comparison of the ^{1}H NMR spectra of [$(TPSH_5)(DCA)_2$] (1.38 ppm), [$(2\text{-}NCH_3CTPPH_3)DCA]^+$ (3.715 ppm; 2-NCH_3-CTPPH is 2-methyl-5,10,15,20-tetraphenyl-2-aza-21-carbaporphyrin)[28] and $Sn^{IV}(TPP)(DCA)_2$ (2.88 ppm)[29] reveals that the C*H*Cl_2 resonances appear in similar upfield regions for three species with different DCA binding (C*H*Cl_2 shift given in parentheses). In these systems the chemical shifts of C*H*Cl_2 are directly related to the geometry dependent ring current effect. Thus, we conclude that the ^{1}H NMR data for [$(TPSH_5^{2+})$-$(DCA)_2$] are consistent with the localization of the DCA^- anion over the centre of the dication in the same way that DCA^- is placed above Sn^{IV} in the $Sn^{IV}(TPP)(DCA)_2$ complex or in the $[(2\text{-}NCH_3CTPPH_3)(DCA)]^+$ ion.[28,29] At the higher DCAH concentration (1 : 50 molar ratio, 203 K) we have detected, in addition to **I**2, two more sets of three singlets at the 0 to −6 ppm region. They resemble the pattern of the most abundant **I**2 species. These resonances are accompanied by well-defined, 27-NH resonances located downfield, with appropriate intensities. Their presence indicates the unexpected formation of the new ionic species **I**2′ and **I**2″. However, in the pyrrole resonance region, only peaks indicating the formation of **P**2 and **I**2 have been seen. Presumably the **I**2′ and **I**2″ pyrrole resonances are hidden under those of **I**2. The spectral pattern of **I**2′ and **I**2″, seen in trace E of Fig. 6, corresponds to the inverted dication because the charactristic marker resonances remained intact. It is important to realize that the

observed changes require at least three different inverted dications in equilibria which also involve the planar **P**2 species. The fundamental equilibria (1) and (2) may be involved in the

$$[(TPSH_5)]^{2+} + DCA^- \rightleftharpoons [(TPSH_5)(DCA)]^+ \quad (1)$$

$$[(TPSH_5)(DCA)]^+ + DCA^- \rightleftharpoons [(TPSH_5)(DCA)_2] \quad (2)$$

anion binding process for both **P** and **I** configurations. The additional processes, which are indicated by the formation of **I**2′ and **I**2″ and the smooth change of the NH chemical shifts for **P**2, suggest also the independent interaction of the dication with the bulk of DCAH through a network of hydrogen bonds. This behaviour resembles that established previously for the new anion-specific binding agent 2-NCH_3CTPPH,[28] where three different dicationic forms have been clearly detected during the titration with DCAH. We have related their formation to lowering of the aromacity of the macrocycle and localization of the positive charge on the protonated nitrogens of the inner perimeter of 2-$NCH_3CTPPH_3^{2+}$. Such a concentration of the electrostatic charge can increase direct interaction of the dication with the counteranion promoting stabilization of ionic pairs.

The titration of $TPSH_3$ with DCAH in [$^2H_6$]DMSO (not shown) resulted in a ^{1}H NMR spectrum for the dication indistinguishable from that established for $TPSH_3$–TFAH in the same solvent, proving that in more polar solvents the formation of tight ionic pairs involving $TPSH_5^{2+}$ is restrained.

Protonation of $TPSH_3$ with HCl

Titration of $TPSH_3$ with HCl (DCl) in [$^2H_2$]dichloromethane solution gave similar results to those obtained for carboxylic acids. On the basis of electronic spectra (not shown) we have found that protonation involves **I**–**P** rearrangements although the respective species do coexist at large ranges of the acid concentration, particularly at 203 K. As was carried out previously, the protonation process has been followed by ^{1}H NMR spectroscopy and these results are shown in Fig. 7. The detected species are formed in the order **I**0→**I**1→**P**2→**I**2 as seems typical for protonation in chlorinated solvents. At higher concentrations of HCl the dicationic forms are involved in complicated equilibria. Their resonances are very broad in the 0 to −6 ppm region and are practically unresolvable for **I**2 species in the pyrrolic region. We have determined the exceptional stabilization of the **I**1 form in comparison to TFAH or DCAH. In this single instance (Fig. 7, traces A and C) we could detect all pyrrole and NH resonances which were observed only partially for **I**1–TFA and **I**1–DCA, respectively. The marked shift differences between **I**1–TFA, **I**1–DCA and **I**1–Cl show that coordination of the counteranion also takes place at the first protonation step.

Interestingly, at very high concentrations of HCl a novel species with strikingly large shifts of NH protons has been formed (Fig. 7, trace E). Tentatively we suggest a new type of the halide–sapphyrin dication adduct although we are not able to determine its structure. The comparable NH shifts were determined for decaalkylated sapphyrin in the presence of a high concentration of HF.[9] There the formation of the dimer or higher aggregates was implied analogously to the presumed dimer of the decaalkyl sapphyrin dication in polar solvents.[6] However in our investigations we found that the formation of sapphyrin aggregates is generally not essential for $TPSH_3$. Anyway, the dimerization process which is feasible for alkylated sapphyrins should be severely limited for $TPSH_{3+n}^{n+}$ due to the steric hindrance of *meso*-phenyl substituents. Such a steric control of the aggregation processes has been well documented for the regular porphyrins, exemplified by comparison of the stacking behaviour of octalkylporphyrins and *meso*-tetraarylporphyrins.[30]

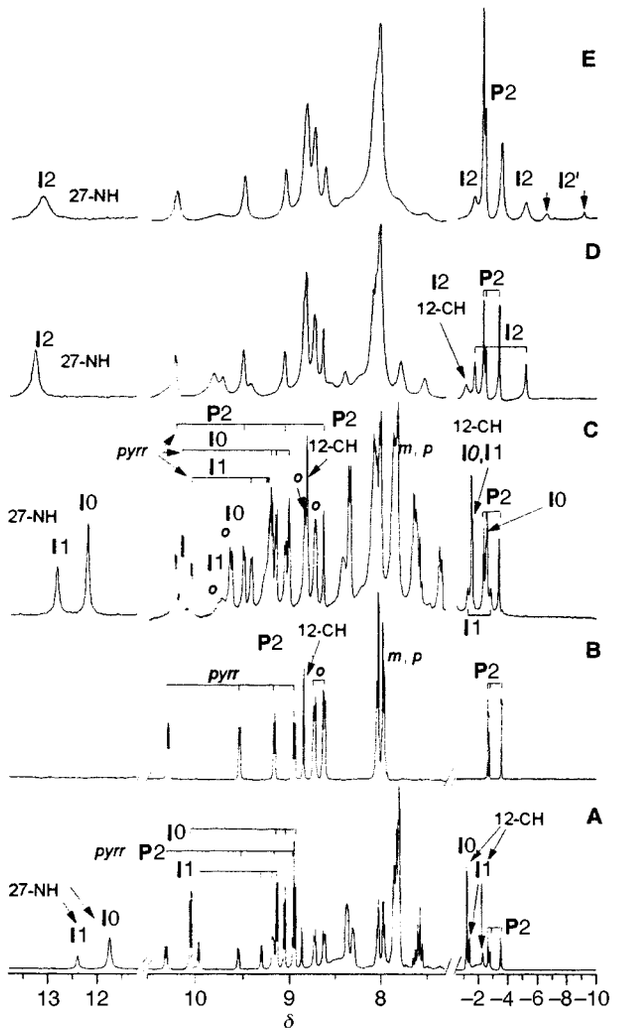

Fig. 7 ^{1}H NMR spectra (300 MHz) of $TPSH_3$: (A) spectrum after addition of 1 μl of HCl ([^{2}H]chloroform, 293 K); (B) spectrum after addition of 66 μl of HCl ([^{2}H]chloroform, 293 K); (C) spectrum after addition of 1 μl of HCl ([$^2H_2$]dichloromethane, 203 K); (D) spectrum after addition of 12 μl of HCl ([$^2H_2$]dichloromethane, 203 K); (E) spectrum after addition of 40 μl of HCl ([$^2H_2$]dichloromethane, 203 K). Saturated solutions of HCl in [^{2}H]chloroform or in [$^2H_2$]dichloromethane have been used for the titrations. Labelling of resonances as described in Fig. 2. The relative intensity of the 0 to −6 ppm and 11 to 15 ppm regions are enhanced to show peaks of the species formed in a small amount.

Conclusions

Considering the available literature data, it seems to be generally accepted that decaalkylated sapphyrins favour the planar geometry of the macrocycle at any protonation level and that the process may be accounted for as outlined in Scheme 2, although the tautomeric equilibria and the molecular structure of **P**0 and **P**1 remain to be directly detected.[9–12] For example, 10 tautomers [(25-NH, 26-N, 27-NH, 28-N, 29-NH), (25-NH, 26-NH, 27-N, 28-NH, 29-N), (25-NH, 26-N, 27-NH, 28-NH, 29-N), (25-N, 26-NH, 27-NH, 28-N, 29-NH), (25-NH, 26-NH, 27-NH, 28-N, 29-N), (25-N, 26-N, 27-NH, 28-NH, 29-NH), (25-NH, 26-NH, 27-N, 28-N, 29-NH), (25-NH, 26-N, 27-N, 28-NH, 29-NH), (25-N, 26-NH, 27-NH, 28-NH, 29-N), (25-N, 26-NH, 27-N, 28-NH, 29-NH)] should be considered in principle at the **P**0 level. (Scheme 2 presumably includes only the more stable structures with a single *cis* arrangement of the NH protons.)

Our systematic ^{1}H NMR studies of 5,10,15,20-tetraphenylsapphyrin have revealed a more intricate nature for sapphyrin protonation, as elaborated in Scheme 1. In essence Scheme 1

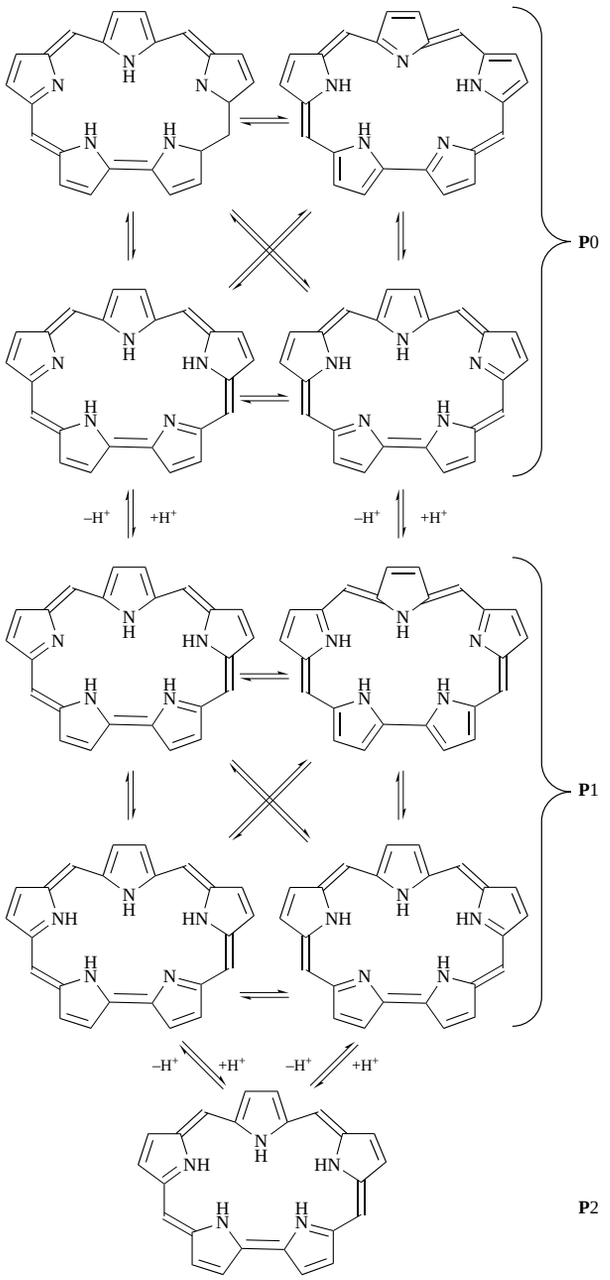

Scheme 2

describes the mechanism found primarily for the inverted structure but which also applies to the planar dication. The **P**2 dicationic form is included either as the final species of titration in DMSO preceded, however, by **I**2 or as an intermediate predecessor of ultimately formed **I**2 in chlorinated solvents. The unusual flexibility of the $TPSH_3$ at different protonation stages does not have any parallel yet in widely investigated pyrrole alkylated *meso* unsubstituted sapphyrins. On the other hand the flexibility of the larger expanded porphyrins was previously documented. The impressive rotations of the two pyrrole units of the hexaphyrin macrocycle were encountered during a palladium amine dichloride coordination.[31] Protonated forms of non-aromatic expanded porphyrins, *i.e.* hexapyrrolic rosarin, decapyrrolic turcasarin[32] or fully conjugated cyclooctapyrrole,[33] demonstrate remarkably twisted conformations.

We have associated the observed rearrangement processes with two fundamental equilibria which involve tetraphenylsapphyrin, *i.e.* protonation of the pyrrolic nitrogens and binding of the anions *via* a system of NH–anion hydrogen bonds. The second factor seems to be of importance in triggering the **I**–**P** rearrangement. The simultaneous binding of two anions may be crucial for the stabilization of the planar structure of $TPSH_5^{2+}$. This condition is fulfilled for a 1:2 molar ratio of $TPSH_3$ to acid in less polar solvents. Accordingly the monocationic species demonstrate an inverted structure. The order of dicationic species formation in [^{2}H]chloroform ([$^2H_2$]dichloromethane) *vs.* [$^2H_6$]DMSO provides an additional argument for the fundamental role of anion binding in determination of the $TPSH_3$ macrocycle structure. When the experiment has been carried out in the polar DMSO environment, which is expected to restrain the ionic pair stabilization, the formation of **I**2 has been favoured over **P**2 even for a low concentration of any investigated acids. The situation changes for a high concentration of carboxylic acid. Here, even for the relatively small anion binding equilibrium constant, a sufficient concentration of anion is provided by effective dissociation in a more polar solvent to force the extended **P**2 structure. The opposite direction of the process has been found in dichloromethane solution for the larger carboxylic acid concentration. The formation of the conglomerate structures of acids, *e.g.* by dimerization, as a competing process may diminish the number of accessible anions once again favouring the inverted structures. Only in the case of the hydrogen chloride titration do both inverted and planar dications coexist in solution. The competing effect suggested for carboxylic acid does not seem to be as important.

In conclusion, 5,10,15,20-tetraphenylsapphyrin presents unique features considering the mechanism of protonation with acid in organic solvents. The geometry of the macrocycle is fully and reversibly controlled by two collaborating factors, *i.e.* protonation of pyrrolic nitrogens and, what is more interesting, anion binding. In fact the inverted–planar sapphyrin conversion can be used as an optically detected sensor of acid and/or anion concentrations.

Experimental

Solvents and reagents

[^{2}H]Chloroform and [$^2H_2$]dichloromethane (Aldrich) were dried by passing over a column of activated basic alumina. TFAH (Aldrich) and DCAH (Ubichem) were used as received.

Preparation of compounds

$TPSH_3$ and [$^2H_{10}$]$TPSH_3$ were synthesised as previously described.[21]

Acid titration

To avoid any possible contamination by traces of DCl/HCl which usually occurs in chlorinated solvents, the ^{1}H NMR samples have to be prepared directly before measurements from the freshly deacidified solvents and thoroughly neutralized 5,10,15,20-tetraphenylsapphyrin. Otherwise the $TPSH_3$ acts as an efficient proton scavenger, showing in the ^{1}H NMR spectrum direct evidence of monocationic species formation (**I**1)Cl. The solution of the acid of interest (trifluoroacetic acid, hydrogen chloride, dichloroacetic acid) in [^{2}H]chloroform ([$^2H_2$]dichloromethane, [$^2H_6$]dimethyl sulfoxide) was titrated by a syringe and the progress of the reaction was followed by ^{1}H NMR spectroscopy. Usually a sample contained 2 mg of $TPSH_3$ in chlorinated solvent. The saturated solution of $TPSH_3$ in [$^2H_6$]DMSO was used.

Instrumentation

^{1}H NMR spectra were measured on a Bruker 300 AMX spectrometer operating in quadrature detection mode. The residual ^{1}H NMR resonances of the deuterated solvents were used as secondary references. Absorption spectra were recorded on a diode array Hewlett Packard 8453 spectrometer.

Acknowledgements

Financial support from the State Committee for Scientific Research KBN of Poland (Grant 3 T09A 14309) is acknowledged with thanks. The quantum mechanic calculations carried out at the Poznań Supercomputer Center (Poznań).

References

1 J. L. Sessler and A. K. Burrell, *Top. Curr. Chem.*, 1992, **161**, 179.
2 (*a*) First reported by R. B. Woodward at the Aromacity Conference, Sheffield, UK, 1966; (*b*) M. M. King, Ph.D. Thesis, Harvard University, Cambridge, MA, USA, 1970.
3 M. J. Brodhurst, R. Grigg and A. W. Johnson, *J. Chem. Soc.*, *Perkin Trans. 1*, 1972, 2111.
4 V. J. Bauer, D. L. J. Clive, D. Dolphin, J. B. Paine III, F. L. Harris, M. M. King, J. Loder, S.-W. Chien Wang and R. B. Woodward, *J. Am. Chem. Soc.*, 1983, **105**, 6429.
5 J. L. Sessler, M. J. Cyr, V. Lynch, E. McGhee and J. A. Ibers, *J. Am. Chem. Soc.*, 1990, **112**, 2810.
6 B. G. Maiya, M. Cyr, A. Harriman and J. L. Sessler, *J. Phys. Chem.*, 1990, **94**, 3597.
7 M. L. Judy, J. L. Matthews, J. T. Newman, H. Skiles, R. Boriack, M. Cyr, B. G. Maiya and J. L. Sessler, *Photochem. Photobiol.*, 1991, **53**, 101.
8 R. Bonnett, *Chem. Soc. Rev.*, 1995, 19.
9 M. Shionoya, H. Furuta, V. Lynch, A. Harriman and J. L. Sessler, *J. Am. Chem. Soc.*, 1992, **114**, 5714.
10 (*a*) J. L. Sessler, M. Cyr, H. Furuta, V. Král, T. Mody, T. Morishima, M. Shionoya and S. Weghorn, *Pure Appl. Chem.*, 1993, **65**, 393; (*b*) J. L. Sessler, M. J. Cyr and A. K. Burrell, *Synlett*, 1991, **3**, 127; (*c*) B. L. Iverson, K. Shreder, V. Král, D. A. Smith, J. Smith and J. L. Sessler, *Pure Appl. Chem.*, 1994, **66**, 845.
11 (*a*) B. L. Iverson, K. Shreder, V. Král and J. L. Sessler, *J. Am. Chem. Soc.*, 1993, **115**, 11 022; (*b*) V. Král, H. Furuta, K. Shreder, V. Lynch and J. L. Sessler, *J. Am. Chem. Soc.*, 1996, **118**, 1595; (*c*) B. L. Iverson, K. Shreder, V. Král, P. Sansom, V. Lynch and J. L. Sessler, *J. Am. Chem. Soc.*, 1996, **118**, 1608.
12 (*a*) V. Král, A. Andrievsky and J. L. Sessler, *J. Am. Chem. Soc.*, 1995, **117**, 2953; (*b*) V. Král, S. L. Springs and J. L. Sessler, *J. Am. Chem. Soc.*, 1995, **117**, 8881.
13 H. Furuta, M. J. Cyr and J. L. Sessler, *J. Am. Chem. Soc.*, 1991, **113**, 6677.
14 J. L. Sessler, H. Furuta and V. Král, *J. Supramol. Chem.*, 1993, **1**, 209.
15 A. Andrievsky and J. L. Sessler, *J. Chem. Soc.*, *Chem. Commun.*, 1996, 1119.
16 L. F. Lindoy, *The Chemistry of Macrocyclic Ligands*, Cambridge University Press, Cambridge, UK, 1989, ch. 5.
17 R. M. Izatt, K. Pawlak, J. S. Bradshaw and R. L. Bruening, *Chem. Rev.*, 1991, **91**, 1721.
18 (*a*) P. Rothemund, *J. Am. Chem. Soc.*, 1936, **58**, 625; (*b*) P. Rothemund, *J. Am. Chem. Soc.*, 1939, **61**, 2912.
19 P. J. Chmielewski, L. Latos-Grażyński, K. Rachlewicz and T. Głowiak, *Angew. Chem.*, 1994, **106**, 805; *Angew. Chem.*, *Int. Ed. Engl.*, 1994, **33**, 779.
20 H. Furuta, H. Asano and T. Ogawa, *J. Am. Chem. Soc.*, 1994, **116**, 767.
21 P. J. Chmielewski, L. Latos-Grażyński and K. Rachlewicz, *Chem. Eur. J.*, 1995, **1**, 68.
22 M. J. Frisch, G. W. Trucks, H. B. Schlegel, P. M. W. Gill, B. G. Johnson, M. A. Robb, J. R. Cheeseman, T. Keith, G. A. Petersson, J. A. Montgomery, K. Raghavachari, M. A. Al-Laham, V. G. Zakrzewski, J. V. Ortiz, J. B. Foresman, J. Cioslowski, B. B. Stefanov, A. Nanayakkara, M. Challacombe, C. Y. Peng, P. Y. Ayala, W. Chen, M. W. Wong, J. L. Andres, E. S. Replogle, R. Gomperts, R. L. Martin, D. J. Fox, J. S. Binkley, D. J. Defrees, J. Baker, J. P. Stewart, M. Head-Gordon, C. Gonzales and J. A. Pople, Gaussian, Inc., Pittsburgh, PA, 1995.
23 (*a*) A. D. Becke, *Phys. Rev. A*, 1988, **38**, 3098; (*b*) C. Lee, W. Yang and R. G. Parr, *Phys. Rev. B*, 1988, **37**, 785; (*c*) B. G. Johnson, P. M. W. Gill and J. A. Pople, *J. Chem. Phys.*, 1993, **98**, 5612; (*d*) A. D. Becke, *J. Chem. Phys.*, 1993, **98**, 5648.
24 W. R. Scheidt and Y. L. Lee, *Struct. Bond.*, 1987, **64**, 1.
25 (*a*) C. B. Storm and Y. Teklu, *J. Am. Chem. Soc.*, 1972, **94**, 53; (*b*) H. J. C. Yeh, M. Sato and I. Morishima, *J. Magn. Res.*, 1977, **26**, 365; (*c*) M. Schlabach, H.-H. Limbach, E. Bunnenberg, A. Y. L. Shu, B.-R. Tolf and C. Djerassi, *J. Am. Chem. Soc.*, 1993, **115**, 4554.
26 M. J. Crossley, L. D. Field, M. M. Harding and S. Sternhell, *J. Am. Chem. Soc.*, 1987, **109**, 2335.
27 (*a*) E. Vogel, M. Köcher, H. Schmicker and J. Lex, *Angew. Chem.*, 1986, **98**, 262; *Angew. Chem.*, *Int. Ed. Engl.*, 1986, **25**, 257; (*b*) B. Wehrle, H.-H. Limbach, M. Köcher, O. Ermer and E. Vogel, *Angew. Chem.*, 1987, **99**, 914; *Angew. Chem.*, *Int. Ed. Engl.*, 1987, **26**, 934; (*c*) J. L. Sessler, E. A. Brucker, V. Lynch, M. Choe, S. Sorey and E. Vogel, *Chem. Eur. J.*, 1996, **2**, 1527.
28 P. J. Chmielewski and L. Latos-Grażyński, *J. Chem. Soc.*, *Perkin Trans. 2*, 1995, 503.
29 D. P. Arnold and J. P. Bartley, *Inorg. Chem.*, 1994, **33**, 1486.
30 (*a*) G. N. La Mar and F. A. Walker, in *The Porphyrins*, ed. D. Dolphin, Academic Press, New York, 1978, vol. 4, p. 140; (*b*) R. V. Snyder and G. N. La Mar, *J. Am. Chem. Soc.*, 1977, **99**, 7178 and references cited therein.
31 R. Charriere, Ph.D. Thesis, University of Fribourg (Switzerland), see ref. 1, p. 246.
32 (*a*) J. L. Sessler, S. J. Weghorn, T. Morishima, M. Rosingana, V. Lynch and V. Lee, *J. Am. Chem. Soc.*, 1992, **114**, 8306; (*b*) J. L. Sessler, S. J. Weghorn, V. Lynch and M. R. Johnson, *Angew. Chem.*, *Int. Ed. Engl.*, 1994, **33**, 1509.
33 E. Vogel, M. Bröring, J. Fink, D. Rosen, H. Schmickler, J. Lex, K. W. K. Chan, Y.-D. Wu, D. A. Plattner, M. Nendel and K. N. Houk, *Angew. Chem.*, *Int. Ed. Engl.*, 1995, **34**, 2511.

Paper 7/02215H
Received 2*nd April* 1997
Accepted 16*th January* 1998